Impact of upstream and downstream constraints on a signaling module's ultrasensitivity

Edgar Altszyler[1,2], **Alejandra Ventura**[2], **Alejandro Colman-Lerner**[2], and **Ariel Chernomoretz**[1,3]

[1]Departamento de Física, Facultad de Ciencias Exactas y Naturales, IFIBA-CONICET, Universidad de Buenos Aires, Ciudad Universitaria, Pabellón 1, Buenos Aires, Argentina. C1428EHA.

[2]Laboratorio de Fisiología y Biología Molecular, Departamento de Fisiología, Biología Molecular y Celular, IFIBYNE-CONICET, Facultad de Ciencias Exactas y Naturales, Universidad de Buenos Aires, Ciudad Universitaria, Pabellón 2, Buenos Aires, Argentina. C1428EHA.

[3]Laboratorio de Biología de Sistemas Integrativa, Fundación Instituto Leloir, Buenos Aires, Argentina. C1405BWE

Abstract

Much work has been done on the study of the biochemical mechanisms that result in ultrasensitive behavior of simple biochemical modules. However, in a living cell, such modules are embedded in a bigger network that constrains the range of inputs that the module will receive as well as the range of the module's outputs that network will be able to detect. Here, we studied how the effective ultrasensitivity of a modular system is affected by these restrictions. We use a simple setup to explore to what extent the dynamic range spanned by upstream and downstream components of an ultrasensitive module impact on the effective sensitivity of the system. Interestingly, we found for some ultrasensitive motifs that dynamic range limitations imposed by downstream components can produce effective sensitivities much larger than that of the original module when considered in isolation.

Keywords

signaling; transfer function; ultrasensitivity; dynamic range

I. Background

Cells continuously sense external and internal cues using specific molecular components in order to elaborate appropriate responses which help to cope with a challenging environment. During the last 15 years, a great deal of experimental and theoretical effort has been devoted to understand the underlying biochemical reaction network responsible for these capabilities. Much of the advance in the field, along with the development of new areas such as synthetic biology, was conceived under a system-level perspective in which signal sensing, transduction, and information processing mechanisms are analyzed in terms of interacting

modules or minimal functional motifs [Tyson *et al* 2003, Benner and Sismour 2005, Alon 2006]. The modular description of molecular biochemical networks is based on the hypothesis that system-level properties may in fact be derived from the analysis of interactions among operationally defined subsets of molecular species, i.e. functional modules [Hartwell *et al* 2000, Kholodenko *et al* 2002, Sneppen *et al* 2010].

Among the plethora of biologically plausible functional units sigmoidal input-output response modules constitute one of the fundamental motifs found in several cellular contexts [Zhang *et al* 2013]. Sigmoidal responses have a threshold input level below which low output signals are produced, and above which high response levels are achieved. The steepness of the transition between low to nearly maximum response is referred to as the module's *sensitivity*. Biochemical modules with steeper transitions than that obtained in a hyperbolic Michaelis-Menten response are called *ultrasensitive* [Goldbeter and Koshland 1981], and in the extreme, they behave like an all or none (digital) switch. At a first approximation, ultrasensitive responses may be described by a Hill equation of the form: $y = A\, x^{n_H}/(EC50^{n_H} + x^{n_H})$, where x and y represent the system's input and output, respectively. The parameter $EC50$ is associated to the input level for which half-maximal output is achieved, A is the maximal output, while n_H is known as the Hill coefficient, and is usually used to quantify the global sensitivity of the corresponding transfer function.

At the molecular level, several mechanisms can produce ultrasensitive or even switch-like responses. For example, under a competition by stoichiometric inhibitor scenario [Ferrell 1996, Buchler and Louis 2008] switch-like responses could arise because the input signal has to overcome the effect of the inhibitors in order to produce appreciable responses. The same kind of mechanism could produce ultrasensitive behavior when translocation sufficiently raises the local concentration of a signaling protein to partially saturate the enzyme that inactivates it [Ferrell 1998]. In covalent cycles, so called zero-order ultrasensitivity could arise when phosphatase and kinases work under saturation and imbalances between phosphorylation and de-phosphorylation rates drive drastic changes in substrate phosphorylation levels [Goldbeter and Koshland 1981]. Multistep activation processes - like multisite phosphorylation [Ferrell 1996, Markevich *et al* 2004, Gunawardena 2005] or ligand binding to multimeric receptors [Rippe 1997] – may also result in ultrasensitive dose-response curves. In these cases, the ultrasensitivity arises as a result of a common regulation of two or more concomitant biochemical processes.

At a system level, sigmoidal modules might be used to implement the switch-like responses that are at the core of cellular decision systems, as well as to provide the necessary nonlinearities upon which more complex behaviors, such as adaptation [Srividhya *et al* 2011], bistability [Angeli *et al* 2004, Ferrell and Xiong 2001], and oscillations [Kholodenko 2000] can emerge. Many theoretical concepts and operational tools for the analysis of the sensitivity features of functional modules have been developed for the analysis of signal propagation through molecular cascades. A module-based analysis of this kind of systems relays on Hartwell's idea of functional modules. They can be conceptualized as discrete entities, composed by different types of molecular species, capable of introducing a well-defined and identifiable functionality into the biochemical system they are embedded on.

Within a modular-based perspective, Goldbeter & Koshland (GK) described in a series of influential contributions sensitivity amplification capabilities of covalent modification cycles, and provided analytical tools to quantify the total amplification in multicyclic cascades [Goldbeter and Koshland 1981, Goldbeter and Koshland 1982]. Rooted in GK's work, a similar framework was presented by Kholodenko *et al* [Kholodenko *et al* 1997] to quantify information transfer in signal transduction pathways. Using concepts borrowed from metabolic control analysis they used *response coefficients*, which describe fractional changes in response levels due to fractional changes in input signals. They showed that, in a multi-level arrangement of consecutive signal processing units (i.e. in a cascade lineup), the global response coefficient equals the product of the response coefficients of each level of the cascade [Kholodenko *et al* 1997, Brown *et al* 1997]. Interestingly, J.E. Ferrell pointed out in a complementary contribution that the overall global sensitivity (assessed by its Hill coefficient *n*) of two consecutive Hill-type modules, could be at most the value obtained by the multiplication of individual module sensitivities (i.e.: $n \le n_1 * n_2$). The actual value depended on the relationship between the first module's output level and the concentration needed to achieve maximal activation of the second module [Ferrell 1997]. As a consequence of this kind of analysis, a classification scheme was coined in terms of the *sub-multiplicative*, *multiplicative* or *supra-multiplicative* character of module-based systems, for cases where the overall system sensitivity, *n*, was found to be lower, equal or larger than the product of the constituent module's ultrasensitivities, n_i. [Racz and Slepchenko 2008, O'Shaughnessy et al 2011].

The very notion of *module* implies that it should be somehow separable from the rest of the system. This separation depends on chemical isolation, which can originate from spatial localization or from chemical specificity [Hartwell *et al* 2000]. For instance, neglecting enzyme-substrate complex formation, a MAPK cascade can be analyzed in terms of three independent modules, characterized by their respective transfer functions, arranged in a linear setup. Importantly, when enzyme concentrations cannot be disregarded, a mechanistic-description that takes into account every possible interaction between cascade molecular components should be considered instead [Ventura *et al* 2008].

As modular-based analysis, mechanistic approaches also support the idea that the biological value of this ubiquitous motifs relies in their ability to convert graded or modestly ultrasensitive responses into markedly switch-like responses. Using a mechanistic model, Ferrell and collaborators could gain system-level insights from their experimental study of steady-state responses of the MAPK cascade in Xenopus oocyte extracts [Huang and Ferrel 1996]. With the aid of their biochemical model they were able to quantify the incremental sensitivity amplification along the cascade levels, and concluded that the cascade arrangement might contribute to the all-or-none character of oocyte maturation.

As already stated, some limitations of the module based description are expected to be found for cases where enzyme concentrations could not be disregarded. Bluthgen et al. showed that, due to sequestration effects (i.e. accumulation of active kinase in complex with its substrate), the *response coefficients* in the Ferrell model [Huang and Ferrell 1996] were lower than expected from the modular-based description of the same cascade [Bluthgen *et al* 2006]. In connection with this behavior, De Racz & Slepchenko analyzed multilevel

cascades of activation-deactivation cycles, and found that the sensitivity lost due to sequestration does not occur when the covalent modification cycles are asymmetric (in particular when phosphatase enzymes are saturated but not the kinases) [Racz and Slepchenko 2008]. Taking into consideration effects like sequestration of shared components[1] [Ventura *et al* 2008, DelVecchio *et al* 2008], it is clear that the integration of a given well-characterized module with upstream and downstream components often alters its information-processing capabilities. This is relevant when trying to understand the behavior of a modular processing unit immersed in its physiological context, or when engineering functional modules for synthetic biology purposes [Ray *et al* 2011, Kittleson *et al* 2012, Ang *et al* 2013].

In the present contribution, we focused on the effect of a specific factor that can qualitatively alter the effective performance of sigmoidal modules, i.e. the actual response dynamic ranges between consecutive modules. In connection with this, Slepchenko and collaborators briefly commented on the effect of a so-called 'misalignment' between two coupled covalent cycles [Racz and Slepchenko 2008]; and along the same lines, Bluthgen et al. [Bluthgen and Herzel 2003] also identified these effects in the case of MAP kinase cascades. Here, we present a general framework that fits these previous observations and that enables a systematic analysis of the system level sensitivities for modules with sigmoidal input-output transfer functions. In particular, we will explore the effective sensitivity of a three-module system as a function of a) the range of inputs that a central sigmoidal module receives from an upstream component (upstream or input constraint), and b) the range of this module's output that a downstream component is able to detect (downstream or readout constraint). As we will show, these constraints on input and readout dynamic ranges can result in effective sensitivities much lower or, quite unexpectedly, larger, than the sensitivity of the original module considered in isolation.

We adopted in this work a deterministic methodology to describe the phenomenology displayed by the analyzed motifs. We acknowledge that the probabilistic character of biochemical reactions could induce non-negligible fluctuations in species concentration in the limit of small number of molecules [Thattai and Van Oudenaarden 2001, Paulsson 2005]. Sensitivity attenuation [Berg 2000, Voliotis 2013], low-pass filtering capabilities in long cascades [Hooshangi 2005], and other interesting noise-related phenomena have already been reported in the literature [Ferrell 1998, Thattai and Van Oudenaarden 2002, Raj and Van Oudenaarden 2009, Ray and Igoshin 2012]. Even though protein fluctuations are ubiquitous in biological systems, we found that our deterministic approach– that becomes accurate whenever proteins are present at large numbers [Berg 2000] – still provide useful insights on the analyzed system's behavior.

The paper was organized as followed. We began with a brief introduction to basic concepts and operational tools used to quantify the sensitivity of general sigmoidal transfer functions. Then, we introduced the considered methodological setup and the relevant parameters used

---

[1]More subtle phenomena, also related to sequestration effects, were reported by Ventura et al [Ventura *et al* 2008]. They proposed a method to deal with the tension that exists between a fully mechanistic and a phenomenological module-based description of a covalent cycle cascade. Using a standard singular perturbation analysis they discovered the presence of a *loading effect* in the cascade that induces an intrinsic negative feedback from each cycle to its predecessor.

in order to quantify input and readout dynamic range restrictions. A detailed analysis of input and output dynamic range constraints on several ultrasensitive sigmoidal motifs is then presented. In the last section, we discussed particular and general observed trends and finally conclusions were drawn.

II. Basics on Sigmoidal response curves

A variety of mechanisms can produce ultrasensitive and even switch-like responses. Even though the detailed shape of each stimulus–response curve differs from mechanism to mechanism, all of them are associated to processes in which, in the vicinity of certain threshold value of the input signal, small relative variations in the stimulus can produce large relative changes in the response.

As we already mentioned, ultrasensitive responses may be described by a Hill equation and even in the absence of any formal mechanistic foundation, this function is widely used as a phenomenological mathematical description of ultrasensitive processes. In general, the following operational definition of the Hill coefficient may be used to calculate the sensitivity of sigmoidal modules:

$$n_H = \frac{\log 81}{\log \frac{x_{0.9}}{x_{0.1}}} \quad [1]$$

where x_r is the signal value producing the r fraction level of maximal response. The Hill coefficient measures the fold increase needed to drive the output from the non-activated state (arbitrarily defined as the 10% of the maximum output) to the fully activated state (defined as the 90% of the maximum output). The *81* value in equation [1] is set to produce a $n_H=1$ for hyperbolic response functions (such as those obtained with simple biochemical reactions that follow the Michaelis-Menten approximation). This means that for this kind of transfer functions, an 81-fold change in input signal is necessary to drive the system output from 10% to 90% of its maximal response. Response functions with n_H values higher than 1 are called *ultrasensitive* responses. They produce the same amount of system's output change, with a much smaller fold change in the input signal (e.g. in a $n_H=2$ case, only a 9-fold input signal increase is needed to achieve the aforementioned level of change in the output level).

It is worth noting that, differently from the paradigmatic Hill function case, many signaling motifs display non-symmetrical response functions. As will be further discussed in next sections, this kind of transfer functions could arise in many relevant biochemical contexts such as in covalent modification cycles, multistep activation modules, and when molecular titration or stoichiometric inhibition are dominant processes in a particular bio-molecular motif.

For covalent cycles described by Goldbeter-Koshland equations, imbalance in enzyme saturation levels induces asymmetries in the sensitivity before and after the *EC50* value [Uribe *et al* 2007]. In this case transfer functions in which the sensitivity displayed for lower input values is larger than the one observed for high input values, can be observed when the phosphatase is in saturation but not the kinase (see Sup Mat SM1) [Uribe *et al* 2007]. Motifs

involving molecular titration mechanisms are also relevant examples of this kind of non-symmetrical response functions. In these units ultrasensitivity could arise when the inhibitor exists in a large quantity and the signaling molecule has a higher binding affinity for the inhibitor than for the target molecule [Buchler and Louis 2008, Zhang et al 2013]. A small increase in signaling molecule concentration cause an explosive response when free inhibitor molecules, forming inactive complexes, are exhausted. This produces a much larger sensitivity for input values below the EC50 input level, than for large input signals, for which a smoother saturation behavior is observed.

Here we proposed to extend the sensitivity quantification provided by equation [1], in order to provide a better characterization of these kinds of non-symmetrical response functions. In this way, left, n_H^L, and right, n_H^R, Hill coefficients can be defined as:

$$n_H^L = \frac{\log 9}{\log \frac{x_{0.5}}{x_{0.1}}}, \; n_H^R = \frac{\log 9}{\log \frac{x_{0.9}}{x_{0.5}}} \quad [2]$$

Left, *symmetric,* or *right-ultrasensitivity* behaviors can then be distinguished and associated to n_H^L/n_H^R values larger, equal or lower than one, respectively. In the same way that dose-response curves with symmetric ultrasensitivity are usually describes by Hill functions, asymmetric ultrasensitivity functions could be adjusted by a pricewise Hill function,

$$F(x) = \begin{cases} A \dfrac{x^{n_H^L}}{EC50^{n_H^L} + x^{n_H^L}} \; if \, x \leq EC50 \\[3mm] A' \dfrac{x^{n_H^R}}{EC50^{n_H^R} + x^{n_H^R}} \; if \, x > EC50 \end{cases}$$

Global sensitivity assessments (equations [1] and/or [2]) do not exhaust the characterization of ultrasensitive sigmoidal curves. A complementary way to quantify the ultrasensitive character of this kind of response curves is given by the response coefficient, *R*, also known as *logarithmic gain* or *elasticity* (term used in metabolic control analysis)[Savageau 1977, Kholodenko *et al* 1997]:

$$R(x) = \frac{x}{y}\frac{dy}{dx} = \frac{d\log y}{d\log x} \quad [3]$$

The response coefficient estimates the local polynomial order of the response, providing a local description of relative changes of input (*x*) and output (*y*) levels.

As shown in figure S1 for several examples, quantities such as the polynomial order of the response function (equation [3]) and/or sensitivity asymmetries (equation [2]) can be used to unveil and quantify differences between diverse ultrasensitive responses. As we will discuss below, these differences in local sensitivity features are extremely relevant and have noticeable consequences when dynamic range constraints are considered on a given module.

III. Upstream and downstream restrictions

Sigmoidal response modules may be found in many different cellular contexts, integrated with diverse upstream and downstream components. In this section we present a simple setup designed to quantify how the sensitivity of the combined system is affected by constraints imposed on the effective input and output dynamic range of the ultrasensitive module (see figure 1).

In order to focus our analysis on effects exclusively due to dynamic range restrictions on the analyzed ultrasensitive unit, hyperbolic responders were chosen as upstream and downstream components of the three module system.

Transfer functions like the ones considered in our analysis present two characteristic concentration scales: one associated to its *EC50* value and the other to its maximum response level, *Omax*. As can be easily appreciated from Figure (2a), both quantities provide natural scales that may determine the ultimate behavior emerging from the interaction between the ultrasensitive module under analysis and its input and output (readout) components. The interplay between these relevant concentration scales of consecutive components can be described by upstream, Q_{up}, and downstream, Q_{down} *restriction coefficients*, defined as follows:

$$Q_{up} = \frac{EC50_M}{\text{Omax}_{up}} \qquad Q_{down} = \frac{Omax_M}{EC50_{down}} \qquad [4]$$

where *Omax* represents the maximum output level and *M*, *up* and *down* subscripts refer to parameters of the ultrasensitive module, upstream component and downstream component respectively.

For small values of Q_{up} the full input dynamic range of the ultrasensitive module is explored by the output generated by the upstream component. Similarly, for small values of Q_{down} the saturation of the downstream component occurs at output concentrations well beyond the central module's maximum output. Hence, when both, Q_{up} and Q_{down} display values much lower than one, the interaction of the upstream and downstream components with the sigmoidal central module is linear and the overall system's sensitivity is expected to be the same as that of the central module in isolation (left panel of figure 2).

On the other hand, large values of the upstream restriction coefficient Q_{up} imply that the central module's EC50 is much larger than the maximum output concentration produced by the upstream component. As can be seen from the example depicted in the center panel of figure 2, a severe reduction in the central module's effective working range (i.e. the range of inputs that would actually stimulate it) could take place when $Q_{up} \gg 1$ and $Q_{down} \ll 1$. In this case, we will say that the module is in an *upstream saturation* or *upstream limited* regime. Considering the toy model introduced in figure 1b, this would correspond to a situation in which the upstream module's maximum response ($Omax_{up} = [B_T]$,) activates only a small amount of [C]. In this case, $Omax_{up}$ would be lower than the input needed by the ultrasensitive module's to achieve its half maximum response (i.e. $Omax_{up} \ll EC50_M$) resulting in $O_{up} \gg 1$.

Finally, large values of the downstream restriction coefficient, Q_{down}, correspond to setups where the central module's maximum output is much larger than the EC50 of the downstream component. In cases like the one depicted in the right panel of figure 2, where $Q_{down} \gg 1$ and $Q_{up} \ll 1$, the range of different outputs of the central module cannot be fully "read" by the downstream unit, and thus its readout range could be severely limited. In this case we will say that the module is in a *downstream saturation* or *downstream limited* regime. In the presented toy model this would occur whenever a small amount of [C^*] is enough to fully activate [D]. This scenario will corresponds to the case in which the maximum module's output is much higher than the ultrasensitive module's input needed to achieve the half maximum response ($Omax_M \gg EC50_{down}$) and hence $Q_{down} \gg 1$ (a quantitative characterization of upstream and downstream saturation regimes is provided in Suplementary Material SM2 for the case of a Hill module).

IV. Analysis of constrained ultrasensitive modules

In either *downstream* or *upstream saturation* scenarios, input and readout processes can constrain the explored dynamic range of the sigmoidal module, making local sensitivity features of the analyzed transfer function become relevant to understand the overall system behavior. To illustrate this point, in this section we present a systematic analysis of the sensitivity of generic ultrasensitive responders coupled to input and readout hyperbolic modules, under different dynamic range restriction conditions. We start by analyzing the case where the ultrasensitive central module's response function is described by a Hill-type mathematical form. We then proceed to extend the analysis to several ubiquitous ultrasensitive motifs, whose ultrasensitive transfer functions can be derived from the corresponding mechanistic models.

A. Hill-type modules

The use of Hill mathematical forms to fit experimental data is a fairly common practice. It is then worth studying the impact of input and readout dynamic range restrictions in this case (without loss of generality we will consider an $n_H=3$ ultrasensitive Hill module).

We start our analysis writing down the expression of the overall system's output as a function of the input signal, *O(I)*, calculated through a simple mathematical composition of the respective single-module transfer functions:

$$O= \underbrace{Omax_{down} \frac{Q_{down}}{Q_{down}+1}} \frac{y^{n_H}}{(1+y)^{n_H}\frac{Q_{up}{}^{n_H}}{1+Q_{down}}+y^{n_H}} = \tilde{O}max_{down} \frac{y^{n_H}}{(1+y)^{n_H}k^{n_H}+y^{n_H}} \quad [5]$$

where $\tilde{O}max_{down}=Omax_{down} \frac{Q_{down}}{Q_{down}+1}$, $\kappa= \frac{Q_{up}}{\sqrt[n_H]{1+Q_{down}}}$ and $y= \frac{I_{up}}{EC50_{up}} I_{up}$ is the input signal of the upstream hyperbolic module (i.e. the input signal for the entire system).

Using equations [5] and [1], we obtained the following analytical expression for the system's Hill coefficient, η:

$$\eta(q_{down}, Q_{up}, n_H) = \frac{\log 81}{\log(\frac{y_{90}}{y_{10}})} = \frac{\log 81}{\log \frac{(10+9\kappa^{-n_H})^{1/n_H} - 1}{(\frac{10}{9}+\frac{1}{9}\kappa^{-n_H})^{1/n_H} - 1}} \quad [6]$$

where y_{10} and y_{90} are the y values which produces the 10% of $\tilde{O}max_{down}$ and 90% of $\tilde{O}max_{down}$ in equation [5].

Figure 3a shows the dependency of the system's overall sensitivity η on parameter κ given by equation [6]. It can be observed that increasing κ results in a loss of the system sensitivity, up to a point where for κ 1, the range-constraint effect is fully developed and the global system achieves its minimal sensitivity. Noticeably, for $\kappa \ll 1$ the global sensitivity equals that of the central Hill module.

Equation [6] reveals that for this particular system the effect of upstream and downstream restrictions on the system sensitivity is in fact a function of a single parameter, κ. Noticeably, this parameter is proportional to the Q_{up} restriction coefficient, but decreases with increasing Q_{down} values. In this way, for this kind of modules, upstream restrictions degrade the module sensitivity level whereas downstream restrictions tend to preserve it. In order to further analyze this result it is worthy to describe the system behavior as a function of Q_{up} and Q_{down} coefficients. In addition this would allow us to establish meaningful comparisons with the analysis of other ultrasensitive motifs, for which an analytic expression cannot be easily obtained.

In figure 3b we present a color-coded systematic characterization of the Hill module's effective sensitivity, numerically estimated using equation [1] as a function of Q_{up} and Q_{down} coefficients. A $\kappa(Q_{down}, Q_{up}) = 1$ line was included in the panel (gray line) to delineate the (upper) area of severe ultrasensitivity reduction.

It can be observed that in the absence of dynamic range restrictions (Q_{down} and $Q_{up} \ll 1$, bottom-left area of figure 3b) the system's estimated sensitivity equals that of the central module. This is the expected behavior from figure 3a as in this case $\kappa \ll 1$.

On the other hand, as expected from equation [6] and the κ dependency on Q_{up} and Q_{down}, parameters, it can be recognized from figure 3b that upstream and downstream constraints have different effects on the system behavior. For a given Q_{down} level, a clear diminution of the system's sensitivity can be observed for setups displaying increasing values of the upstream restriction coefficient Q_{up}. On the contrary, for a given Q_{up} value, a rise in the downstream restriction coefficient value Q_{down}, corresponds to a decrease in the κ parameter level, and results in an increase system's sensitivity levels.

Analysis of highly constraint situations—Analytical expressions for the overall response function can be obtained for highly constraint situations (i.e. when $Q_{up} \gg 1$ and/or $Q_{down} \gg 1$). The dynamic range effectively spanned by the Hill's module when input and/or readout saturation takes place in this system is actually limited to the module's low input region (see Sup. Mat SM3, and figure 2). In any of these saturation scenarios the central module response function can be approximated by:

$$O_M = Omax_M \frac{I_M^{n_H}}{EC50_M^{n_H} + I_M^{n_H}} \sim Omax_M \frac{I_M^{n_H}}{EC50_M^{n_H}} \quad [7]$$

with I_M, the input signal of the analyzed central module M.

As we show in Suplementary Material SM2, when equation [7] is a valid approximation, the readout unit restricts the module's effective working range whenever $Q_{down} \gg Q_{up}^{n_H}$. In this case the condition $\kappa \ll 1$ is satisfied and no sensitivity reduction is expected to take place in the system. Accordingly, for situations where the downstream component's output reaches saturation, and the upstream module works in its linear regime (i.e. I_{up} spans the linear region of the upstream module's transfer function, see Sup Mat SM2 for mathematical details) the input unit's response function can be approximated by $O_{up}(I_{up}) \sim Omax_{up}I_{up}/EC50_{up}$, and the whole system transfer function results in

$$O_{down}(O_M(O_{up}(I_{up}))) \sim O_{down}^{max} \frac{y^{n_H}}{\sigma^{n_H} + y^{n_H}} \quad [8]$$

where $y = \frac{I_{up}}{EC50_{up}}$ and $\sigma = \frac{Q_{up}}{\sqrt[n_H]{Q_{down}}}$. Equation [8] shows that under this regime, when it is the readout module the only one that saturates, the system responds as a Hill function with $\eta = n_H$. The analyzed situation corresponds to the right-bottom corner of figure 3b where, as expected, the numerically estimated η value was found to be close to n_H.

On the other hand, saturation takes place at the upstream unit whenever $Q_{up} \gg \sqrt[n_H]{Q_{down}}$ (see Sup. Mat. SM2). This corresponds to κ getting values larger than one, and the system is expected to achieve its minimal sensitivity level (see figure 3a). In this case the upstream module saturates and the downstream readout module, on the contrary, operates nearly in the linear regime, so we can speak of an *upstream saturation* regime. The response function of the downstream readout module can be approximated by $O_{down}(I_{down}) \sim Omax_{down}I_{down}/EC50_{down}$, and the entire system transfer function can be expressed as

$$O_{down}(O_M(O_{up}(I_{up}))) \sim \frac{Omax_{down}}{\sigma^{n_H}} \left[\frac{y}{1+y} \right]^{n_H} \quad [9]$$

Equation [9] does not have the general Hill functional form. Instead, powers of y of orders between *0* and *n* now appear in the denominator, resulting in a drop of the system's effective sensitivity, in concordance with the behavior expected from figure 3a. This working regime corresponds to the entire upper area in figure 3b, where the condition $Q_{up}^{n_H} \gg Q_{down}$ holds (see Sup. Mat SM2 and SM4).

B. The general sigmoidal case for constraint situations

The above-presented analysis may be easily generalized to sigmoidal response functions that, as the Hill mathematical function case, could be approximated in the low input signal range (i.e. in the input's range actually covered under a downstream/upstream limited situation) by

$$O_M \sim A I_M^n \quad [10]$$

Here n is a positive constant that equals the mean polynomial order of the transfer function for small input signals, and A is a proportionality constant.

Whenever equation [10] holds, equations [8] and [9], valid for downstream and upstream saturation situations respectively, can be recast into the following expressions:

$$O_{down}(O_M(O_{up}(I_{up}))) \sim Omax_{down} \frac{y^n}{\frac{Omax_M}{AEC50_M^n} \frac{Q_{up}^n}{Q_{down}} + y^n} \quad [11]$$

$$O_{down}(O_M(O_{up}(I_{up}))) \sim \frac{Omax_{down}}{\frac{Omax_M}{AEC50_M^n} \frac{Q_{up}^n}{Q_{down}}} \left[\frac{y}{1+y}\right]^n \quad [12]$$

It is worth noting that it is the mean polynomial order exhibited at low input ranges, n, and not the Hill coefficient, n_H, of the analyzed transfer functions, what affects the system's effective sensitivity value.

Equation [11] states that the overall system response is of the Hill function mathematical form, but importantly, it has $\eta = n$ (and not n_H) as its Hill exponent. Importantly, this means that downstream saturation could produce *super-multiplicative* behavior for transfer functions which present low-input polynomial order values, n, larger than the overall displayed ultrasensitivity, n_H (i.e. satisfying $n > n_H$).

Left and right ultrasensitivities are related to the global Hill coefficient by the following simple expression that holds for the general case:

$$\frac{2}{n_H} = \frac{1}{n_H^L} + \frac{1}{n_H^R}$$

As the global Hill coefficient n_H is the harmonic mean of left and right coefficients, it will be biased towards the minimum value between n_H^L and n_H^R. Hence, for left-ultrasensitive transfer functions (for which $n_H^L > n_H^R$), it is expected that $n \sim n_H^L > n_H$ hold for them. Therefore, left-ultrasensitive units are in principle capable to display supra-multiplicative behavior under downstream constraint situations. As will be further explored in the next sections this last observation is particularly relevant for several biochemical motifs with left-ultrasensitivity, like: asymmetric Goldbeter-Koshland modules, and titration-based and multistep-activation ultrasensitive units.

C. Goldbeter-Koshland modules

The term *ultrasensitivity* was originally coined by Goldbeter and Koshland (GK) to describe amplification sensitivity capabilities displayed by covalent modification cycles, such as phosphorylationdephosphorylation [Goldbeter and Koshland 1981] (see figure 4). For these

systems, GK derived an analytical expression of the corresponding response function (i.e. the GK response function) valid when enzymes are in much lower concentration than their substrates. Moreover, they showed that a substantial increase of the system's sensitivity can be observed when both, kinases and phosphatases, are saturated. Given the prominent role played by this motif as a building block of signaling cascades, this way of generating ultrasensitivity - termed zero-order ultrasensitivity mechanism– has received a lot of attention [Ferrell 1996, Racz and Slepchenko 2008, O'Shaughnessy *et al* 2011].

In order to analyze the effect of dynamic range limitations on this important motif, we considered a GK ultrasensitive module where both, kinase and substrate, were equally saturated (without loss of generality we fixed the system's parameters to achieved an $n_H=3$). For this ultrasensitive module we proceeded to numerically estimate using equation [1] the overall system's sensitivity, η, in different upstream and downstream constraint scenarios (figure 5a).

As in the above analysis, when input and/or readout saturation effects were noticeable, the module's effective working range was constrained to its low input signal region (see figure 2). However, in this case, the polynomial order of the GK transfer function tends to $n=1$ for low enough input signals (see Figure S1b). As a consequence, there is now a loss of sensitivity not only for *upstream limited* regimes, when the input module saturates, but also for large values of Q_{down}, in the *downstream limited* regime (right-bottom region of figure 5a).

It is interesting to consider the case of asymmetric GK ultrasensitive functions, where only one of the enzymes is saturated (i.e. either the phosphatase is saturated and not the kinase or the kinase is saturated and not the phosphatase), producing *left* or *right-ultrasensitive* response curves (see Sup Mat SM1). Right and symmetric cases exhibit no differences in their qualitative behavior (figure 5b). However noticeable differences arise in the effect of constraints on the central module's dynamic range for the case of a *left-ultrasensitive* GK function (figure 5c). As for the symmetric case, a loss of sensitivity can be observed for *upstream limited* regimes (upper area of figure 5c). However, for intermediate downstream saturation levels in absence of upstream saturation (bottom-center in figure 5c) a strong increase in sensitivity can be observed. In this regime, the readout range encompasses the most sensitive part of the left-ultrasensitive curve, increasing the effective system's sensitivity. For higher values of the downstream restriction coefficient, the module's effective output dynamic range is further reduced, the polynomial first order nature of the response becomes dominant (n=1), and the system's sensitivity is severely lost reaching $\eta = 1$ (bottom-right in figure 5c).

D. Multistep activation modules

In a multistep activation module, a common input signal simultaneously regulates more than one biochemical process that synergistically produces an output response [Zhang *et al* 2013]. These motifs are relevant in many biological situations, for instance for multiple distributive phosphorylation processes [Gunawardena 2005] or in the context of gene regulation, when the promoter region of a transcription factor's target gene has multiple binding sites [Rippe 1997]. We analyze here an instance of the latter scenario, but equivalent

conclusions could be drawn for multiple phosphorylation systems in the limit of non-saturated reactions [Gunawardena 2005].

We proceed by considering the biochemical scheme of reactions taking place inside the transcriptional module shown in figure 6, where, for the sake of simplicity, we assumed that there are only two *cis*-regulatory response elements. In this scheme *A* is the transcription factor, and *B* the associated transcribed mRNA.

Assuming mass action kinetics, the steady state module's transfer function can be written as:

$$O_M(A) = \frac{1}{\delta} \frac{\nu_1 K_2 A + \nu_2 A^2}{K_1 K_2 + K_2 A + A^2} \quad [13]$$

where $K_i = k_i^- / k_i^+$ is the equilibrium dissociation constant for the ith binding site. In the case where $\nu_1 \sim 0$ (i.e. protein transcription can be neglected for single-site binding) the module can achieve the maximal sensitivity value, $n_H=2$, in the limit of $K_1 \gg K_2$, which corresponds to high cooperativity between binding sites [Rippe1997]. On the other hand, for $K_1 \ll 1$ the response tends toward a hyperbolic functional form presenting $n_H=1$.

It is worth noting that the polynomial order (i.e., the response coefficient) of the transfer function given by equation [13] in the low input region is quadratic. As we have described above, this implies that under a *downstream restriction* regime, this module could achieve an effective sensitivity of $\eta_H \sim 2$. Notably, this arises directly from a structural property of the module, independently of the particular choice of its internal parameter values. This means that even in the case of no-cooperativity (for instance, if K_1 and K_2 were of the same order) maximal ultrasensitivity may be achieved in the regime where the readout module saturates. We show in figure 7a the transfer function corresponding to equation [13], for a choice of internal parameter values compatible with a module sensitivity level of $n_H=1.36$.

The response function presents a *left-ultrasensitive* character (with $n_H^L=1.55$ and $n_H^R=1.21$). In fact, for low input signals the module can display sensitivity levels larger than $n_H=1.36$ $(n=2)$, and consequently the overall system's sensitivity could increase under downstream restrictions. To illustrate this point, in figure 7b we show the analysis of the three module system's sensitivity. As expected, it can be appreciated that for large values of the *downstream restriction coefficient*, a sensitivity level of $\eta = 2$ can be achieved, similarly to what it could have been obtained from an isolated module displaying high levels of cooperativity.

E. Competition modules

Molecular titration and stoichiometric inhibition processes can lead to left-ultrasensitive behavior if an inhibitor *B* is abundant and has high affinity for a signaling species *A* [Ferrell 1996, Buchler and Louis 2008, Rowland *et al* 2012]. At low values of total A, all of it is in the form of an inactive complex B:A. This will be true up to the point where all *B* is consumed by the complex. At this threshold point all the buffering capacity of B is exhausted and a small signal increment, A, will be almost entirely available for activating a downstream target, leading to a sizeable increase in the response function. As an example of this type of ultrasensitive motif we studied a simple model of protein sequestration and

transcriptional response proposed by Buchler and Cross [Buchler and Cross 2009] (see figure 8).

According to the Buchler and Cross model (see Sup. Mat. SM5) the equilibrium concentration of a transcription factor A, that can reversibly bind to a stoichiometric inhibitor B, can be expressed as:

$$A = \frac{A_T - B_T - K_d + \sqrt{(A_T - B_T - K_d)^2 + 4A_T K_d}}{2} \quad [14]$$

where A_T and B_T are total concentrations of the signaling and inhibitor species, respectively. $K_d = k_1^-/k_1^+$ is the reaction dissociation constant, given as a ratio of the backward and forward kinetic constants, k_1^- and k_1^+, respectively. In addition, A can also bind to a single DNA-binding site, activating a transcriptional response at a rate O. If basal transcription can be disregarded, the steady state system's transcriptional response is given by

$$O = O_{max} \frac{A}{\in + A} \quad [15]$$

where $\varepsilon = k_2^-/k_2^+$ is the EC50 of the hyperbolic response function and O_{max} is the maximal induced mRNA transcription rate (see Sup. Mat. SM5 for details).

We show in figure 9 the corresponding module response function, $O = O(A_T)$, for a case where the buffering effect of B is expected to be sizable ($K_d/B_T << 1$). The input-output curve has a marked threshold for $A_T \sim B_T$ (around a value of 100 in figure 9a). The module's transfer function is strongly left asymmetric ($n_H = 2$, $n_H^L = 3.7$, $n_H^R = 1.4$). This implies that if a downstream readout module imposed constraints on the effective dynamic range, the left-ultrasensitive character of the module response function could be exploited to obtain a large sensitivity for the complete constrained system.

It is important to point out that the left Hill coefficient is also a global measure, and might not reflect the existence of much higher levels of local sensitivity (see Sup Mat SM1). This is indeed the case here, and the reason why, even though the left Hill coefficient is only 3.7, an overall effective sensitivity of about 12 may be obtained for this system in a downstream restriction regime. This is reported in figure 9b, where up to a six-fold global sensitivity increase can be observed for mild downstream limited regimes (bottom-center region of figure 9c).

F. Arrangement of two covalent cycles

In this section we aim to illustrate how the concepts introduced so far could be used to analyze more general setups in which dynamic range misalignments could also play a major role in connection with the ultrasensitive character of the system

Slepchenko and collaborators showed that linear arrangements of covalent cycles acquire a Hill sensitivity that exceeds the multiplicative limit for situations where activators are much less saturated than inhibitors [Racz and Slepchenko 2008]. In this regime, sequestration effects are negligible, and we can use our general framework to analyze the supra-

multiplicative behavior they reported. Moreover, it is worth noting that in these asymmetrical configurations the corresponding transfer functions present a markedly left-ultrasensitive character suggesting that the observed increase in sensitivity could be explained in terms of read-out dynamic range restrictions operating on the composed system.

In order to evaluate this possibility, we numerically generated an ensemble of asymmetric bicyclic covalent cascades using the same parameter sampling procedure used by Slepchenko in [Racz and Slepchenko 2008]. For each cascade instance we considered the second module as the read-out unit of the first one, and estimated the corresponding downstream restriction coefficient values, Q_{down} (see Sup. Mat. SM6 for details). In addition, we assessed the observed supra-multiplicative character of the system defining the

oversensitivity coefficient: $\pi = n_H^{cascade}/(n_H^{cycle})^2$, which is larger, lower or equal to 1 when the two cycles combines supramultiplicatively, submultiplicatively or multiplicatively respectively. For the sake of completeness, relevant features of the considered model, and of the sampling procedure are summarized in the supplemental material SM6.

We found (green points in figure 10) that supra-multiplicative behavior ($\pi > 1$) occurs for almost every cascade realization when the analysis was constrained to exactly the same subspace of parameters (see Sup. Mat. SM6 for details) that was explored by Slepchenko and collaborators in [Racz and Slepchenko 2008]. It can be recognized from the figure that the sampled realizations spanned mild *downstream restriction coefficient* values. When we relaxed some of the constraints of the original sampling methodology (see Sup. Mat. SM6) a wider interval of Q_{down} could be spanned (blue points in figure 10) revealing a non-monotonous behavior of $\pi = \pi(Q_{down})$.

The observed peak in the oversensitivity is entirely compatible with the behavior reported for mild *downstream limited* scenarios found in the two downstream constraint left-ultrasensitive response functions: asymmetric GK cycles and competition modules (see bottom part of figures 5c and 9b). These findings suggest that the behavior of the overall sensitivity level of the compound system could be understood in terms of the downstream restriction concepts introduced in this paper.

V. Discussion and Conclusion

Despite the success of module-based approaches to disentangle the complexity of cellular biochemical networks, on a general basis, care should be taken when realistic, integrated systems are analyzed, to accommodate the cases where the properties of individual components change upon interconnection.

In the present contribution we asked if the simplest possible non-trivial form of distortion by interconnection, i.e. limitations on the input and/or output effective working ranges of a given module imposed by upstream and downstream components, could produce substantial changes to the ultrasensitive features of a sigmoidal module.

We made use of a three-module setup, and considered the case where different ultrasensitive modules of interest were coupled to Michaelis-Menten-type modules, acting as input and read-out components. We evaluated the overall system sensitivity considering, for each analyzed case, different working-range *misalignment* situations assessed in terms of upstream and downstream *restriction coefficients*, Q_{up} and Q_{down}.

We found that, independently from the detailed mechanism involved, whenever the upstream module acts as the limiting component (i.e. large Q_{up} values), the global ultrasensitivity character of the system is severely reduced. On the other hand, we found a much richer dependency of the overall system's ultrasensitivity on the downstream restriction coefficient, Q_{down}. Whenever the downstream unit is the limiting element of the cascade (i.e. for large Q_{down} *values*, and small Q_{up} values) different behaviors arise depending on the specific non-linearities displayed by the analyzed ultrasensitive module (GK vs Hill, for example).

In the light of these results, downstream dynamic range restrictions should be particularly taken into consideration when analyzing modules presenting left-ultrasensitive responses. We already analyzed molecular titration modules based on a threshold model of transcription presented by Buchler and Cross [Buchler and Cross 2009]. In a recent analytical study, Gunawardena found that ordered distributive multisite phosphorylation systems could also have response functions of the same mathematical form than the one depicted in figure 9a (compare this figure with figure 2 in Gunawardena's work [Gunawardena 2005]). He reasoned that this kind of transfer function creates an efficient threshold. The system response is maintained close to 0, for input signals below a suitable threshold (*input 100* in the case of figure 9). However, above the threshold, the response does not switch between 0 and 1 abruptly, as would be the case for an efficient switch. In this context, it is worth noting that, even though such a module could be considered a *bad switch* when working in isolation, a downstream-limited readout unit could easily convert it into a good switch taking advantages of the local non-linearities of the module's response curve, as was demonstrated in figure 9b for the competition module.

In addition, our general framework allowed us to analyze distinctive features displayed by specific biochemical motifs. For instance we noticed that, irrespectively of their specific degree of cooperativity, multistep activation modules could produce high levels of sensitivity under downstream limited regimes. Interestingly, when left-ultrasensitive transfer functions were involved, the system overall ultrasensitivity could be significantly enhanced for relatively mild downstream constrained situations. For these cases, one may imagine that the downstream component's EC50 value is *fine-tuned*, in the sense that only the most sensitive part of the sigmoidal module's output is read by the downstream unit just before it reaches its saturation levels. In this way, downstream saturation could be considered as a new mechanism on its own, capable of building a highly ultrasensitive device, from an original asymmetrical and modestly ultrasensitive module.

Supplementary Material

Refer to Web version on PubMed Central for supplementary material.

Acknowledgments

References

Alon, U. An Introduction to systems Biology. London, UK: Chapman & Hall; 2006.

Ang J, Harris E, Hussey BJ, Kil R, McMillen DR. Tuning Response Curves for Synthetic Biology. ACS Synthetic Biology. 2013; 2:547–567. [PubMed: 23905721]

Angeli D, Ferrell JE, Sontag ED. Detection of multistability, bifurcations, and hysteresis in a large class of biological positive-feedback systems. PNAS. 2004; 101(7):1822–1827. [PubMed: 14766974]

Berg OG, Paulsson J, Ehrenberg M. Fluctuations and quality of control in biological cells: zero-order ultrasensitivity reinvestigated. Biophys J. 2000; 79(3):1228–1236. [PubMed: 10968987]

Benner SA, Sismour AM. Synthetic Biology. Nat Rev Genet. 2005; 6(7):533–543. [PubMed: 15995697]

Birtwistle MR, Rauch J, Kiyatkin A, Aksamitiene E, Dobrzynski M, Hoek JB, Kolch W, Ogunnaike BA, Kholodenko BN. Emergence of bimodal cell population responses from the interplay between analog single-cell signaling and protein expression noise. BMC Systems Biology. 2012; 6:109. [PubMed: 22920937]

Bluthgen N, Herzel H. How robust are switches in intracellular signaling cascades. Journal of theoretical Biology. 2003; 225:293–300. [PubMed: 14604583]

Bluthgen N, Bruggeman FJ, Legewie S, Herzel H, Westerhoff HV, Kholodenko BN. Effects of sequestration on signal transduction cascades. FEBS Journal. 2006; 273:895–906. [PubMed: 16478465]

Brown GC, Hoek JB, Kholodenko BN. Why do protein kinase cascades have more than one level? Trends Biochem Sci. 1997; 22(8):288. [PubMed: 9270298]

Buchler NE, Louis M. Molecular titration and ultrasensitivity in regulatory networks. J.Mol.Biol. 2008; 384:1106–1119. [PubMed: 18938177]

Buchler NE, Cross FR. Protein sequestration generates a flexible ultrasensitive response in a genetic network. Mol Syst Biol. 2009; 5:272. [PubMed: 19455136]

Constante M, Grunberg R, Isalan M. A biobrick library for cloning custom eukaryotic plasmids. PLoS One. 2011; 6(8):e23685. [PubMed: 21901127]

Chang JT, Carvalho C, Mori S, Bild AH, Gatza ML, Wang Q, Lucas JE, Potti A, Febbo PG, West M, Nevins JR. A Genomic Strategy to Elucidate Modules of Oncogenic Pathway Signaling Networks. Mol Cell. 2009; 34(1):104–114. [PubMed: 19362539]

Del Vecchio D, Ninfa A, Sontag E. Modular cell biology: retroactivity and insulation. Mol Sys Biol. 2008; 4:161. p161.

Elf J, Ehrenberg M. Fast evaluation of fluctuations in biochemical networks with the linear noise approximation. Genome Res. 2003; 13(11):2475–2484. [PubMed: 14597656]

Ferrell JE. Tripping the switch fantastic: how a protein kinase cascade can convert graded inputs into switch-like outputs. Trends Biochem. Sci. 1996; 21:460–466. [PubMed: 9009826]

Ferrell JE. How responses get more switch-like as you move down a protein kinase cascade. Trends Biochem Sci. 1997; 22(8):288–289. [PubMed: 9270299]

Ferrell JE, Machleder EM. Science. 1998; 280(5365):895–898. [PubMed: 9572732]

Ferrell JE. How regulated protein translocation can produce switch-like responses. Trends in Biomedical Sciences. 1998; 23(11):461–465.

Ferrell JE. Life Sciences: 1–6. Encyclopedia Life Sciences. 2001 http://dx.doi.org/10.1038/npg.els. 0001407.

Ferrell JE, Xiong W. Bistability in cell signaling: How to make continuous processes discontinuous, and reversible processes irreversible. Chaos. 2001; 11(1):227–236. [PubMed: 12779456]

Goldbeter A, Koshland DE. An amplified sensitivity arising from covalent modification in biological systems. PNAS. 1981; 78(11):6840–6844. [PubMed: 6947258]

Goldbeter A, Koshland DE. Sensitivity amplification in biochemical systems. Q Rev Biophys. 1982; 15(3):555–591. [PubMed: 6294720]

Gunawardena J. Multisite protein phosphorylation makes a good threshold but can be a poor switch. PNAS. 2005; 102(41):14617–14622. [PubMed: 16195377]

Hartwell LH, Hopfield JJ, Stanislas Leibler S, Murray AW. From molecular to modular cell biology. Nature. 402(6761 Suppl):C47–C52. [PubMed: 10591225]

Hooshangi S, Thiberge S, Weiss R. Ultrasensitivity and noise propagation in a synthetic transcriptional cascade. Proc Natl Acad Sci U S A. 2005; 8(10):3581–3586. 102. [PubMed: 15738412]

Huang C-YF, Ferrell JE. Ultrasensitivity in the mitogen-activated protein kinase cascade. Proc. Proc. Natl. Acad. Sci. 1996; 93:10078–10083.

Kholodenko BN, Hoek JB, Westerhoff HV, Brown GC. Quantification of information transfer via cellular signal transduction pathways. FEBS Letters. 1997; 414:430–434. [PubMed: 9315734]

Kholodenko BN. Negative feedback and ultrasensitivity can bring about oscillations in the mitogen-activated protein kinase cascades. Eur J Biochem. 2000; 267:1583–1588. [PubMed: 10712587]

Kholodenko BN, Kiyatkin A, Bruggeman FJ, Sontag E, Westerhoff HV, Hoek JB. Untangling the wires: a strategy to trace functional interactions in signaling and gene networks. Proc Natl Acad Sci. 2002; 99(20):12841–12846. [PubMed: 12242336]

Kittleson JT, Wu GC, Anderson JC. Successes and failures in modular genetic engineering. Current Opinion in Chemical Biology. 16:329–336. [PubMed: 22818777]

Kollmann M, Lovdok L, Bartholomé K, Timmer J, Sourjik V. Design principles of a bacterial signaling network. Nature. 2005; 438:504–507. [PubMed: 16306993]

Markevich NI, Hoek JB, Kholodenko BN. Signaling switches and bistability arising from multisite phosphorylation in protein kinase cascades. Journal Cell Biology. 2004; 164(3):353.

O'Shaughnessy EC, Palani S, Collins JJ, Sarkar CA. Tunable signal processing in synthetic MAP kinase cascades. Cell. 2011; 7(1):119–131. 144. [PubMed: 21215374]

Papin JA, Hunter T, Palsson BO, Subramaniam S. Reconstruction of cellular signalling networks and analysis of their properties. Nat. Rev. Mol Cell Biol. 2005; 6:99–111. [PubMed: 15654321]

Paulsson J. Models of stochastic gene expression. Physics of Life Reviews. 2005; 2:157–175.

Racz E, Slepchenko BM. On sensitivity amplification in intracellular signaling cascades. Phys. Biol. 2008; 5:036004–036012. [PubMed: 18663279]

Raj A, Van Oudenaarden A. Nature, Nurture, or Chance: Stochastic Gene Expression and Its Consequences. Cell. 135:216–226. [PubMed: 18957198]

Ray JC, Tabor JJ, Igoshin OA. Non-transcriptional regulatory processes shape transcriptional network dynamics. Nat Rev Microbiol. 2011; 9(11):817–828. [PubMed: 21986901]

Ray JC, Igoshin OA. Interplay of gene expression noise and ultrasensitive dynamics affects bacterial operon organization. PLoS Comput Biol. 1012; 8(8):e1002672. [PubMed: 22956903]

Rowland MA, Fontana W, Deeds EJ. Crosstalk and competition in signaling networks. Biophys J. 103(11):2389–2398. [PubMed: 23283238]

Rippe K. Analysis of protein-DNA binding in equilibrium. B.I.F. Futura. 1997; 12:20–26.

Registry of Standard Biological Parts. (http://partsregistry.org).

Savageau. Biochemical systems analysis. Addison-Wesley Pub. Co; 1997.

Sneppen K, Krishna S, Semsey S. Simplified Models of Biological Networks. Annu Rev Biophys. 2010; 39:43–59. [PubMed: 20192769]

Srividhya J, Li Y, Pomerening JR. Open Cascades as Simple Solutions to Providing Ultrasensitivity and Adaptation in Cellular Signaling. Phys Biol. 2011; 8(4):046005. [PubMed: 21566270]

Thattai M, Van Oudenaarden A. Noise in gene regulatory networks. Proc Natl Acad Sci. 2001; 98(3): 8614–8619. [PubMed: 11438714]

Thattai M, Van Oudenaarden A. Attenuation of Noise in Signaling Cascades. Biophysical J. 2002; 82:2943–2950.

Tyson JJ, Chen KC, Novak B. Sniffers, buzzers, toggles and blinkers: dynamics of regulatory and signaling pathways in the cell. Curr Opin Cell Biol. 2003; 15(2):221–231. [PubMed: 12648679]

Gomez-Uribe C, Verghese GC, Mirny LA. Operating regimes of signaling cycles:statics, dynamics, and noise filtering. PLoS Comput Biol. 2007; 3(12):e246. [PubMed: 18159939]

Ventura AC, Sepulchre JA, Merajver SD. A hidden feedback in signaling cascades is revealed. PLoS Comput Biol. 2008; 4(3):e1000041. [PubMed: 18369431]

Voliotis M, Perrett RM, McWilliams C, McArdle CA, Bowsher CG. Information transfer by leaky, heterogeneous, protein kinase signaling systems. Proc Natl Acad Sci. 2014; 111(3):E326–E333. [PubMed: 24395805]

Zhang Q, Bhattacharya Sudin, Andersen Melvin E. Ultrasensitive response motifs: basic amplifiers in molecular signalling networks. Open Biol. 2013; 3:130031. [PubMed: 23615029]
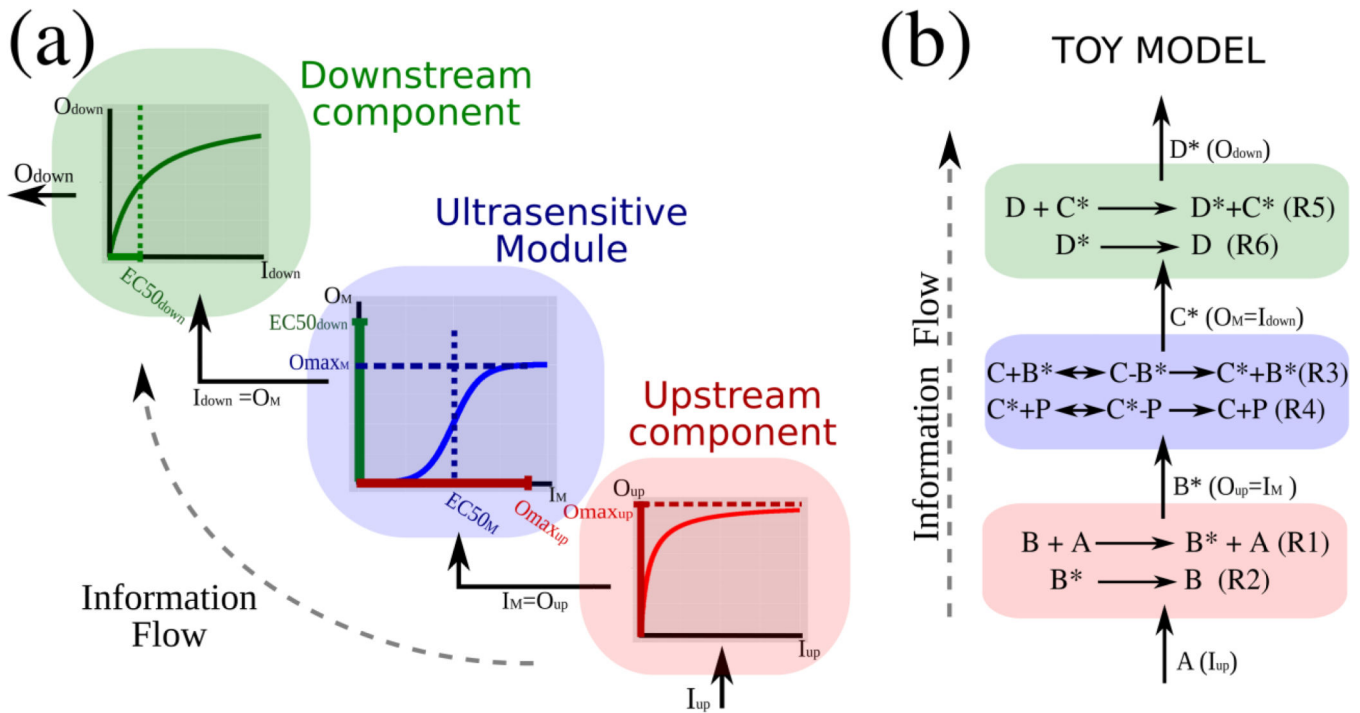
Figure 1.
Panel A) Setup of the extended system used to analyze the effects of the dynamic range limitations imposed by upstream (red) and downstream (green) components on an ultrasensitive module (blue). The maximum output level of the upstream unit, *Omax_up*, sets the extent of the spanned input range of the ultrasensitive module (red horizontal axis on the blue panel). On the other hand, input values, I_{down}, in the sensitive region of the downstream component (i.e. $I_{down} < EC50_{down}$) set the effective readout range of the ultrasensitive module (green vertical axis on the blue panel). Panel B) Representative toy model involving a zero-order ultrasensitive phosphorylation-dephosphorylation module (R3 and R4 biochemical reactions), connected to an upstream catalytic activation unit (R1,R2) and a downstream deactivation hyperbolic units (R5,R6). For this example $I_{up} = [A]$, $O_{up} = I_M = [B^*]$, $O_M = I_{down} = [C^*]$ and $O_{down} = [D^*]$. When sequestration processes between the ultrasensitive module and the upstream component is negligible ($[C - B^*] \ll [B] + [B^*]$ a module-based description can be adopted. The transfer function of upstream and downstream components follow a Michaelis-Menten curve, while the transfer function of the ultrasensitive module follows a G-K function.
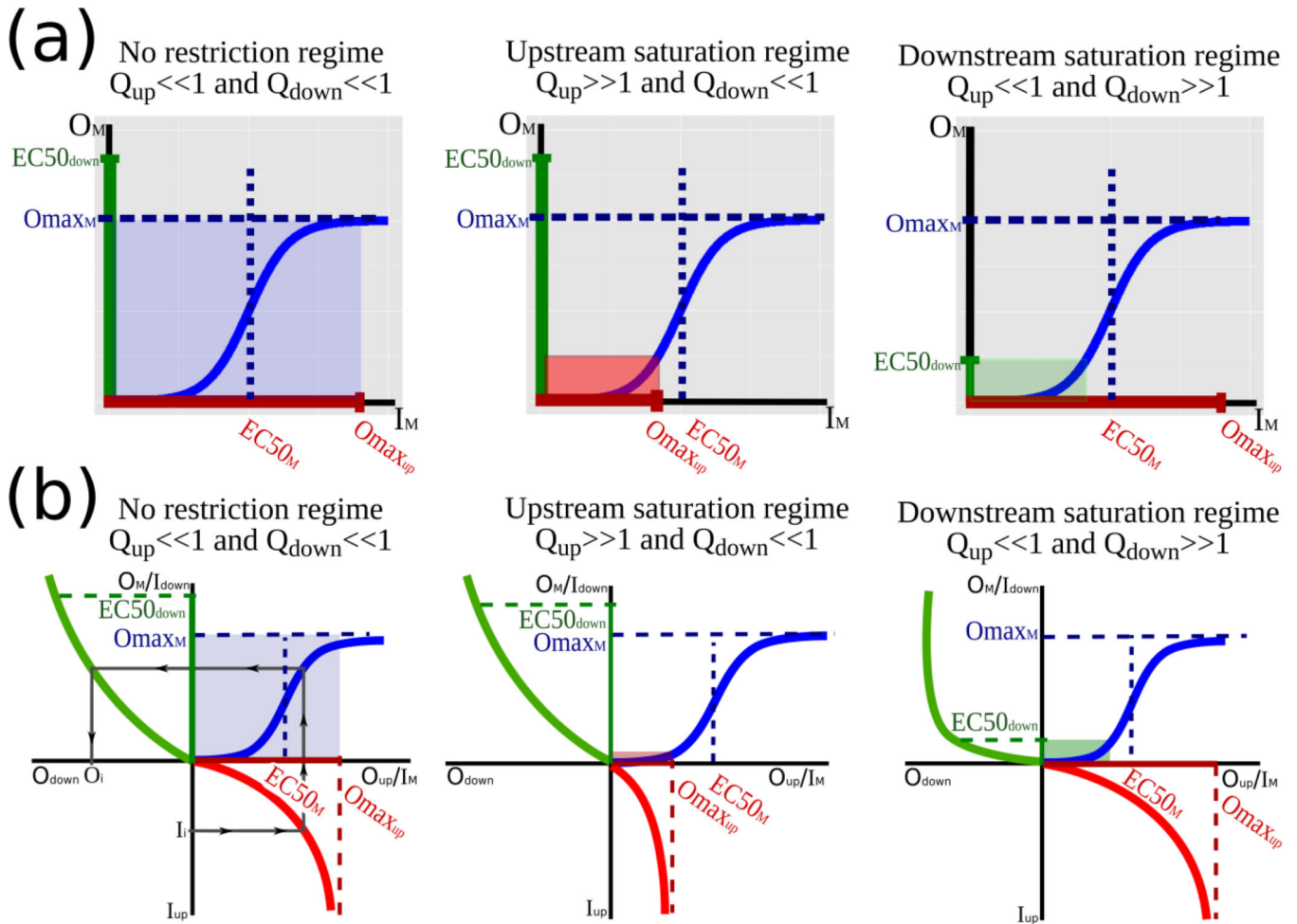
Figure 2.
(a) Schematic response function diagrams for a given ultrasensitive module are shown in left, center, and right panels for no-limitation, upstream limitation, and downstream limitation regimes respectively. In each case a red horizontal and a green vertical line, aligned with panel axis, represent the module's input and read-out operative ranges imposed by upstream and downstream components respectively. The effective module's working ranges are highlighted in each panel. In the left most panel Q_{up}, $Q_{down} <<1$ ($Omax_{up}>EC50_M$ and $EC50_{down}>Omax_M$), and saturation of the input and readout modules do not play a role in the system response. For large values of Q_{up} ($Omax_{up}<EC50_M$) an *upstream saturation* regime can be defined, in which the upstream module's maximum output level do limit the spanned input range of the ultrasensitive module (central panel). On the other hand, large values of Q_{down} ($EC50_{down}<Omax_M$) correspond to *downstream saturation* situations where the readout module limits the effective output range of the ultrasensitive module (rightmost panel). (b) A diagram to illustrate, through graphical composition, how an input signal, $I_{up}=I_i$, is transmitted along the entire system is shown in the left most panel for a non-constraint regime. Transfer functions of the upstream component, ultrasensitive-module, and downstream unit are depicted in the lower-right, upper-right, and upper-left quadrants respectively. The same colors and labels as in panel (a)

were used. Similar diagrams are shown in center and right-most panels for upstream saturation and downstream saturation regimes respectively.
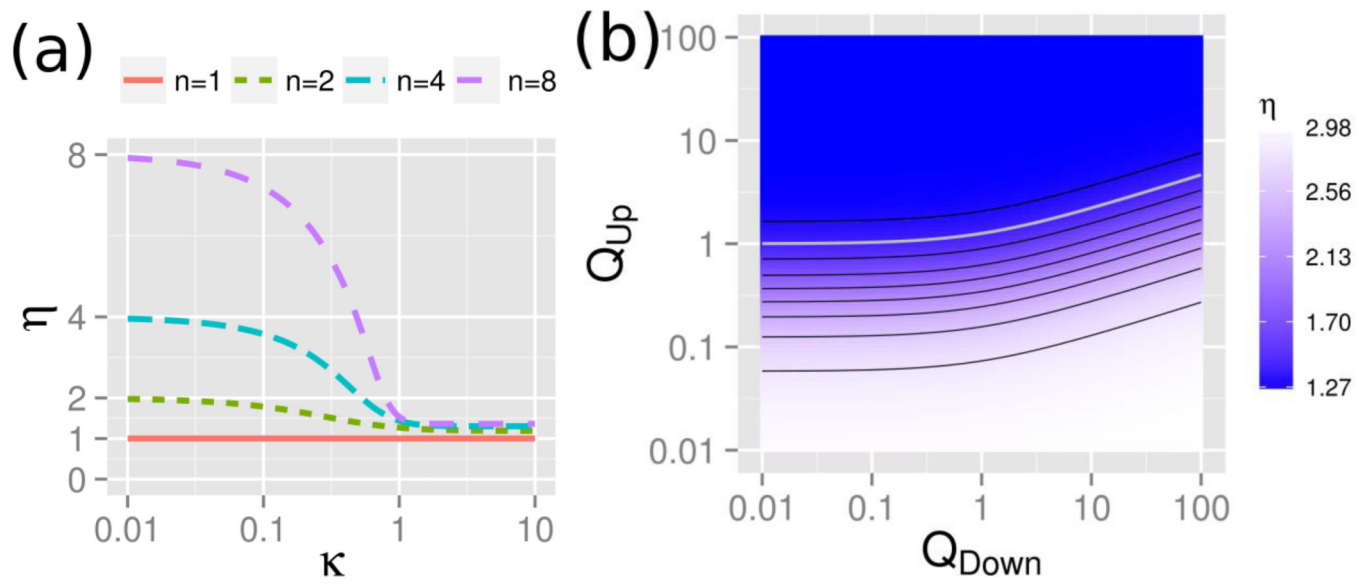
Figure 3.
(a) System's Hill coefficient, η, dependency on the parameter κ (see equation [6]) were estimated for several Hill type ultrasensitive modules. $n_H=1, 2, 4$ and 8 are shown with red, green, light blue and violet colors respectively. It can be seen that for κ>1 the system's sensitivity is strongly attenuated, while for κ<<1 no sensitivity reduction takes place. (b) Heat-maps of system's Hill coefficient (η) as a function of Q_{up} and Q_{down}
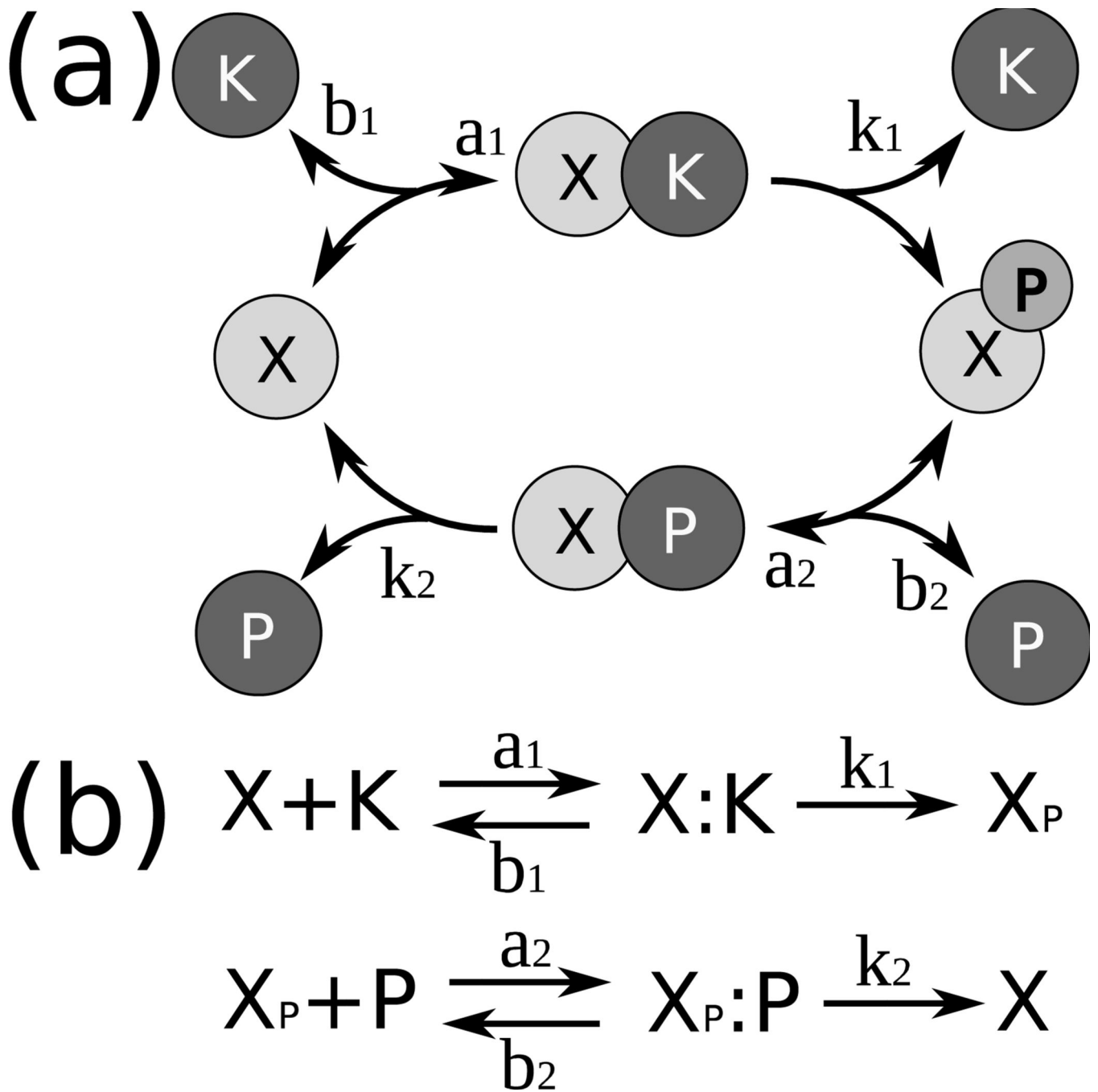
Figure 4.
Goldbeter and Koshland covalent cycle. (a) Scheme, (b) biochemical reactions.
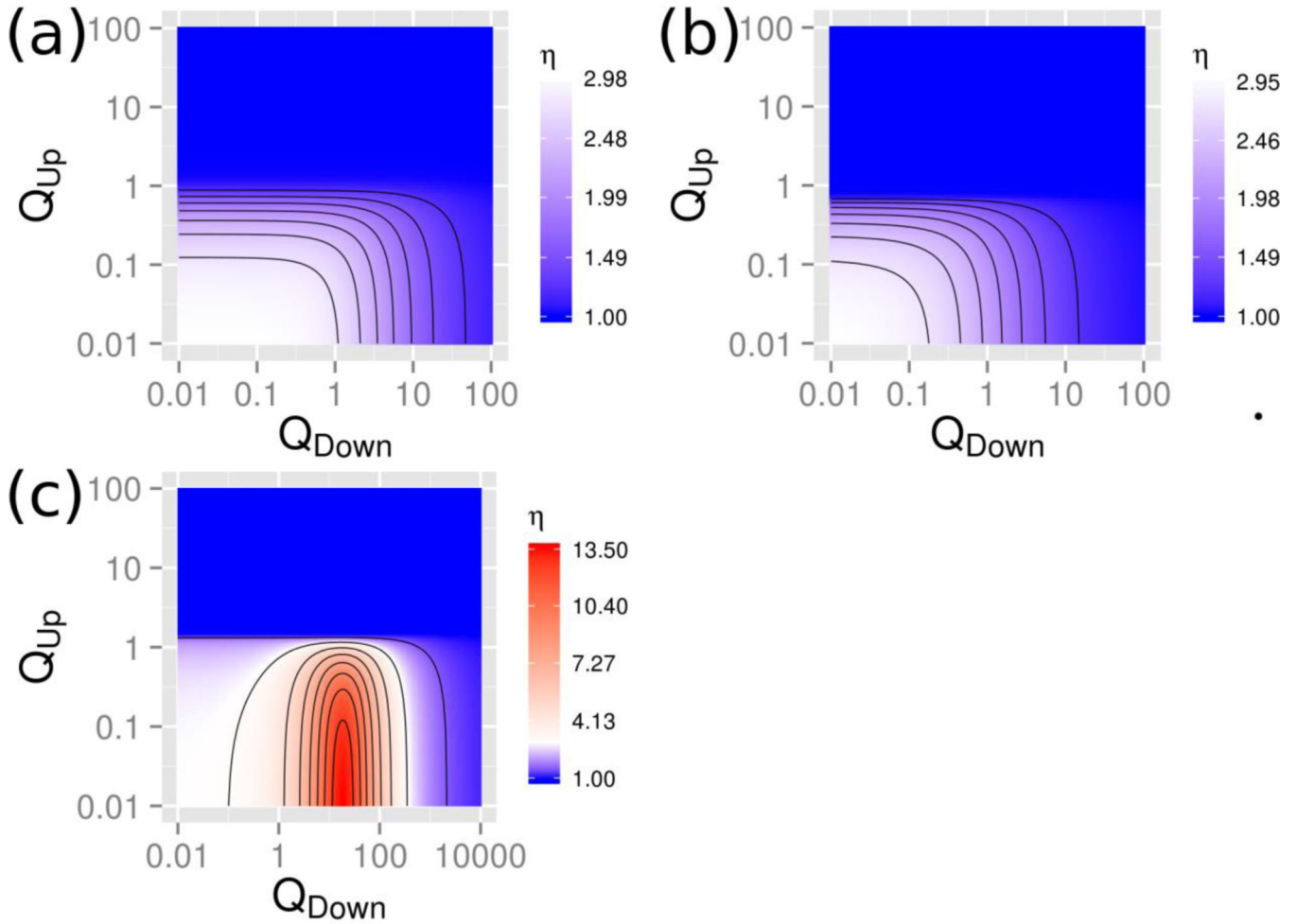
Figure 5.

Heat-maps of Hill coefficient (η) calculated for different GK ultrasensitive modules coupled to input and readout hyperbolic modules for different values of Q_{up} and Q_{down}. (a) Symmetric ultrasensitive GK module, with $\dfrac{k_1 + a_1}{b_1 X_T} = \dfrac{k_2 + a_2}{b_2 X_T} = 0.14$ (b) Right ultrasensitive GK module, with $\dfrac{k_1 + a_1}{b_1 X_T} = 0$ and $\dfrac{k_2 + a_2}{b_2 X_T} = 0.63$ (c) Left ultrasensitive GK module, with $\dfrac{k_1 + a_1}{b_1 X_T} = 0.63$ and $\dfrac{k_2 + a_2}{b_2 X_T} = 0.001$. Transfer functions and response coefficients of these modules in isolation are shown in figure S1. All the panels have the same color code, lines in (a) and (b) represent the same η values, which are different from those in (c).
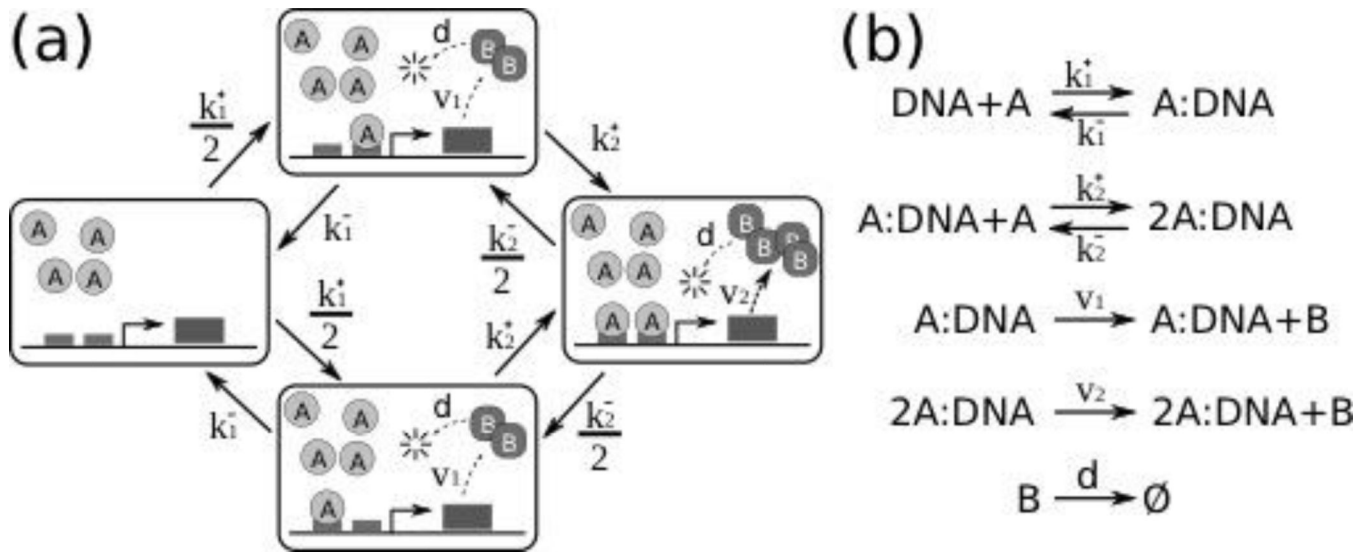
Figure 6.
Simple model of a transcription factor A, which can binds to a promoter with multiple binding sites. (a) Scheme, (b) biochemical reactions.
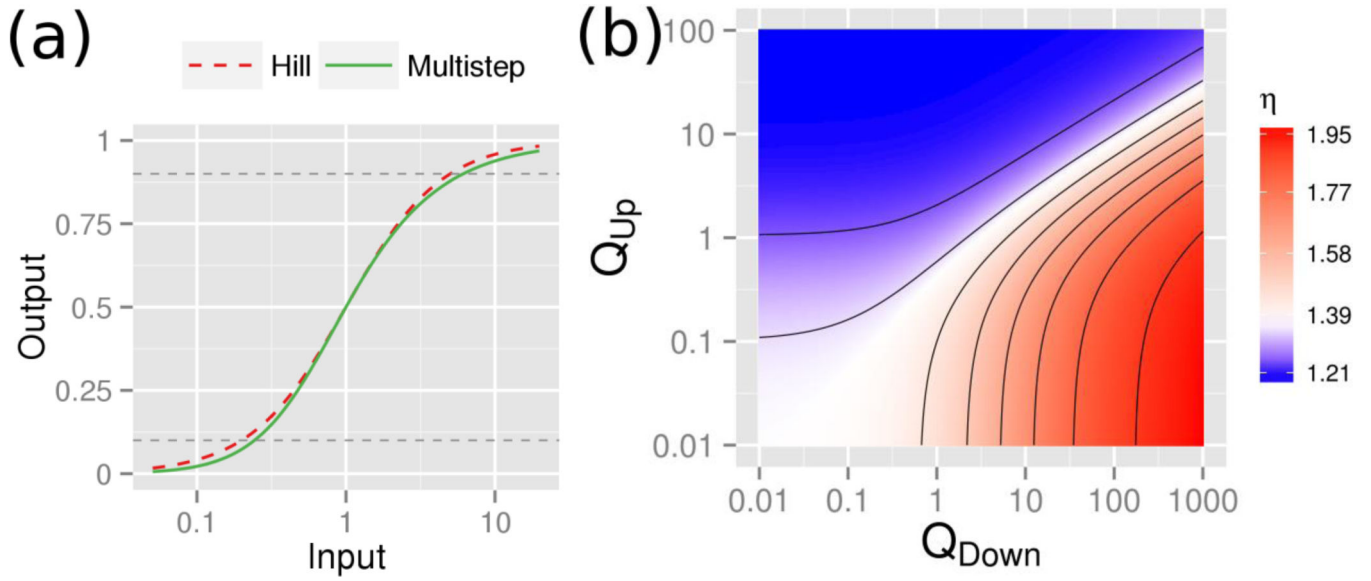
Figure 7.
(a) The transfer function for the multistep activation module (equation [13], with v_1=0 and $v_2 = K_1 = K_2 = \delta = 1$) and a Hill function of the same Hill coefficient, n_{Hill}=1.36, are shown as a green-continuous, and a red-dashed line respectively. Both curves have the same EC50 but the *multistep* green curve lies below the red Hill curve. Therefore, the multistep transfer function presents a higher left-ultrasensitivity coefficient, and a lower right ultrasensitivity coefficient value.

(b) Heat-map for the system's Hill coefficient for the same multistep activation module as panel (a). It can be seen that under downstream saturation ($Q_{down} >> 1$ and $Q_{up} << 1$), the system displays an effective sensitivity value $\eta \sim 2$, as it is expected for a transfer function with a quadratic initial increase.
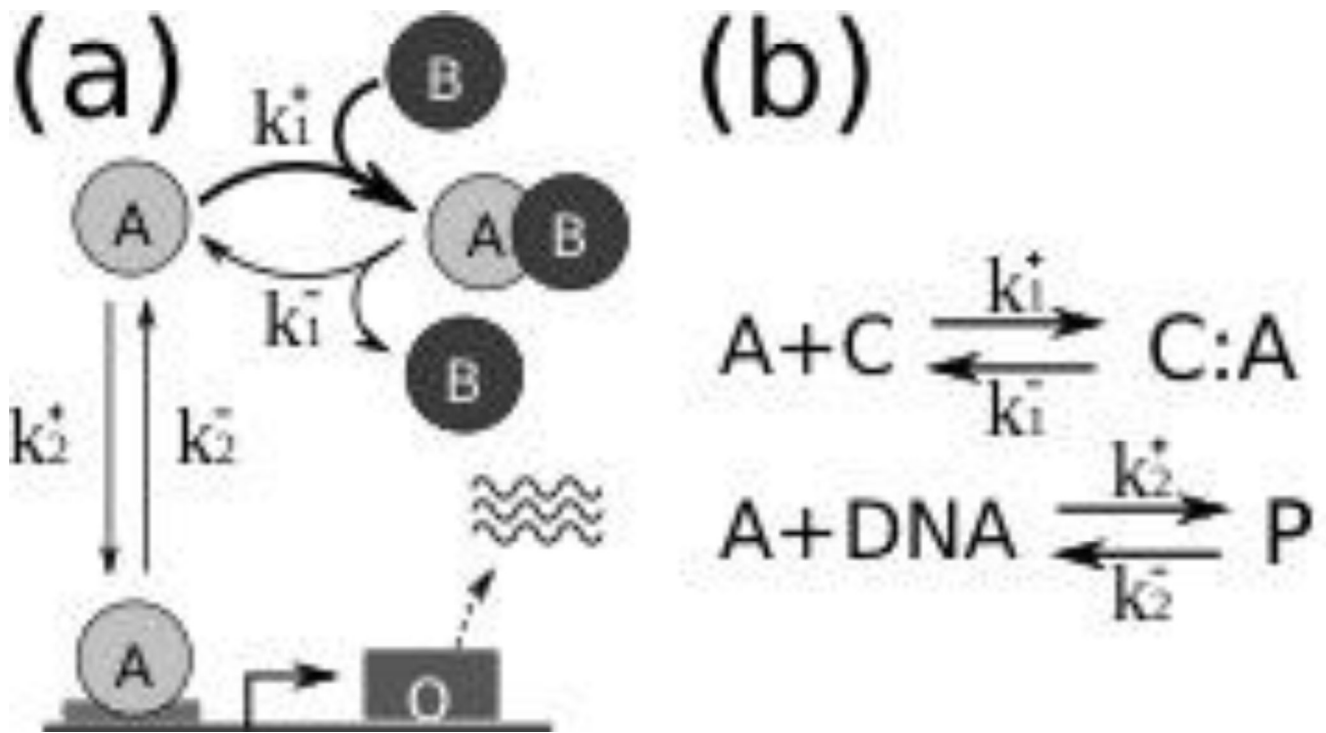
Figure 8.
Simple model of protein sequestration and transcription. Active transcription factor A is sequestered by inhibitor B into an inactive AB complex that cannot bind DNA. (a) Scheme, (b) biochemical reactions.
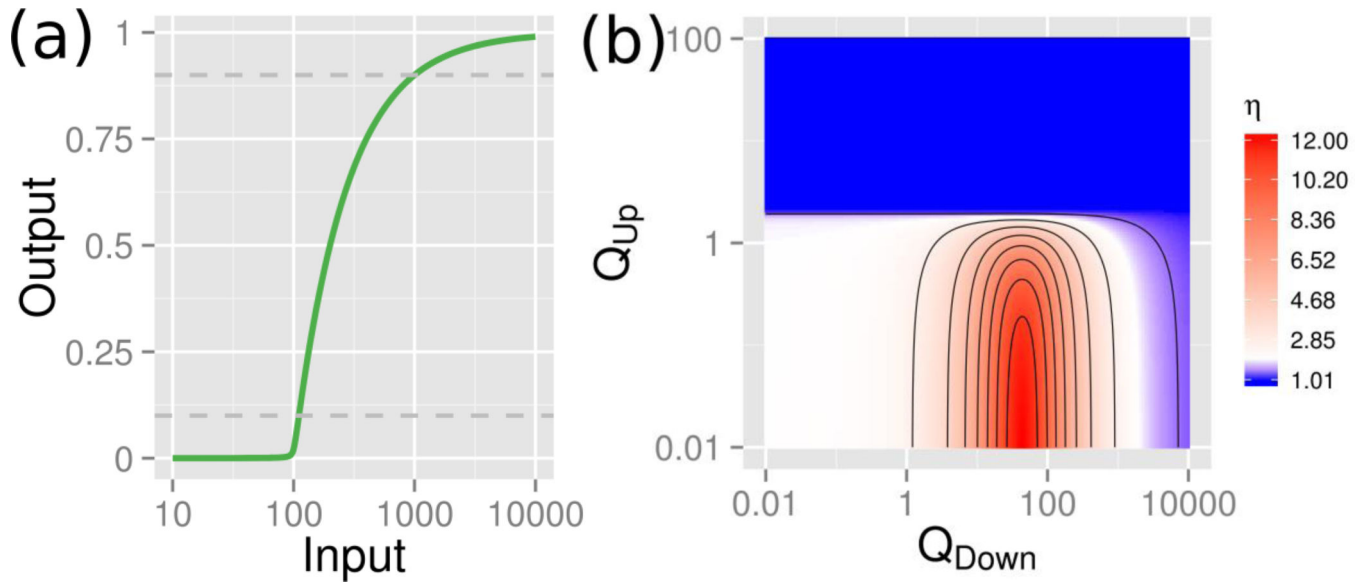
Figure 9.
(a)Transfer function for the competition module, O= O(A_T) (equations [14] and [15]), with $O_{max}=1$, $B_T=100$, $K_d = k_1^-/k_1^+ =0.05$ and $\varepsilon = k_2^-/k_2^+=100$. The high asymmetry observed in terms of left and right ultrasensitivity makes this module a good molecular implementation of a threshold device. In fact The input-output curve has a marked threshold for $A_T \sim B_T$. (b) Heat-map of system's Hill coefficients for a competition module with the same parameters than panel (a). As was the case for other left-asymmetric response functions (e.g. the asymmetric GK case shown in figure 3c) a marked increase in overall global sensitivity arises for mild downstream restrictions. Because of the linear character displayed by the transfer function for low input signal levels, the system sensitivity tends to $\eta=1$ for extremely downstream constraint situations ($Q_{down} \gg 1$ and $Q_{up} \ll 1$).
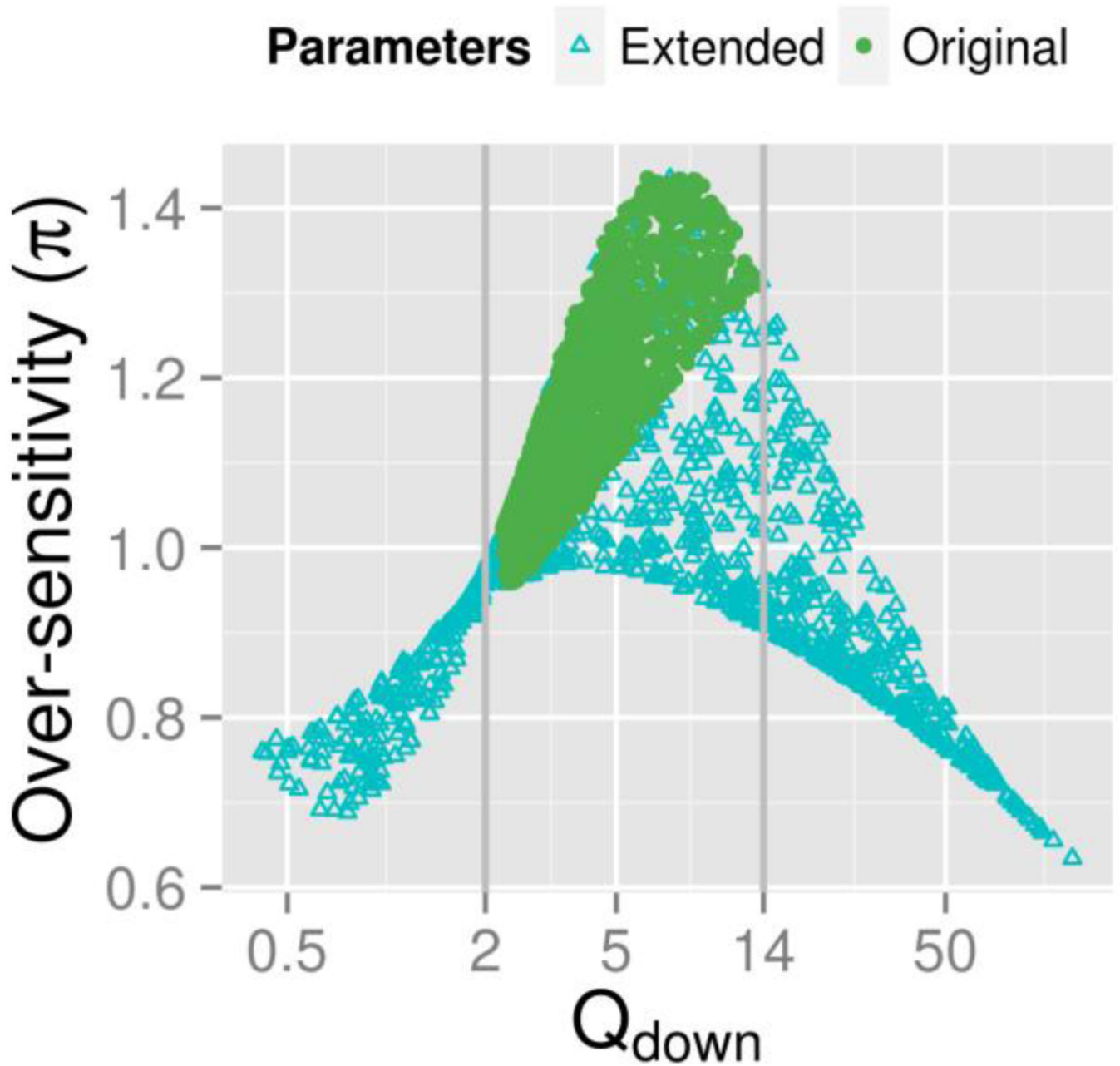
Figure 10.
Over-sensitivity as a function of Q_{down} calculated for an ensemble of 2000 cascades. Green points correspond to 1000 cascade realizations from the original Slepchenko sampling procedure. Points obtained considering an extended interval log(c) in $[-3,-1.2]$ and no restriction on y_{max} value are shown as light-blue points. Vertical lines mark Q_{down} boundaries for which supramultiplicativity is observed for the original Slepchenko sampling. A non-monotonous behavior of $\pi=\pi(Q_{down})$ could be easily recognized for the extended sampling case.